

Kinesin family member 3A inhibits the carcinogenesis of non-small cell lung cancer and prolongs survival

YIE YANG¹, XIAO LIU², RUI LI², MENGJU ZHANG², HONG WANG³ and YIQING QU⁴

¹Department of Clinical Laboratory, Shandong Provincial Qianfoshan Hospital, The First Hospital Affiliated with Shandong First Medical University;

²Department of Pulmonary and Critical Care Medicine, Qilu Hospital, Cheeloo College of Medicine, Shandong University; ³Department of Thoracic Surgery, Shandong Provincial Qianfoshan Hospital,

The First Hospital Affiliated with Shandong First Medical University;

⁴Department of Pulmonary and Critical Care Medicine, Qilu Hospital of Shandong University, Jinan, Shandong 250012, P.R. China

Received December 12, 2019; Accepted August 21, 2020

DOI: 10.3892/ol.2020.12211

Abstract. Kinesin family member 3A (KIF3A) plays a crucial role in the carcinogenesis of different types of human cancer. The present study aimed to identify the role of KIF3A in the carcinogenesis of non-small cell lung cancer (NSCLC). KIF3A protein expression was determined in 163 patients with NSCLC using immunohistochemistry staining. The prognosis of patients with NSCLC was determined using Kaplan-Meier survival and Cox regression analyses. The function of KIF3A on the carcinogenesis and metastasis of NSCLC was determined *in vitro*. Furthermore, a protein-protein interaction (PPI) network of KIF3A was constructed and the potential interacting molecules were identified using bioinformatic analysis. The protein expression levels of KIF3A were significantly lower in the NSCLC tissues compared with that in the adjacent tissues, and low KIF3A expression level was associated with unfavorable survival outcomes in patients with NSCLC. Furthermore, KIF3A knockdown increased proliferation, invasion and metastasis, and inhibited apoptosis of NSCLC cells. KIF3A was demonstrated to interact with intraflagellar transport 57 (IFT57) in the PPI network. In addition, validation analyses indicated that KIF3A mRNA

expression levels were positively correlated with IFT57 mRNA expression levels in clinical NSCLC samples and NSCLC cell lines. Taken together, the results of the present study suggested that KIF3A is a key tumor suppressor gene for carcinogenesis and metastasis of NSCLC, it may also function as a biomarker and interacts with IFT57 in the progression of NSCLC.

Introduction

Lung cancer is one of the most common types of human cancer (11.6% of the total cases) and a major cause of cancer-associated mortality (18.4% of the total cancer mortalities) worldwide (1). Non-small cell lung cancer (NSCLC) accounts for ~85% of all types of lung cancer (2). The major types of NSCLC include lung adenocarcinoma (LUAD, 63%), lung squamous cell carcinoma (LUSC, 30%) and lung large cell carcinoma (7%) (2). Currently, surgical resection is the most beneficial therapeutic strategy for lung cancer (3). Chemotherapy, radiotherapy and targeted drugs are also extensively used; however, the therapeutic resistance of these drugs is a major cause of treatment failure. Thus, understanding the underlying molecular mechanisms for carcinogenesis is important for the development of successful therapy in treating lung cancer.

Kinesin family member 3A (KIF3A) is a motor protein, that is essential for the formation and functional mechanisms of cilia (4-6). It has been reported that KIF3A plays a central role in the initiation and maintenance of medulloblastoma (7) and a key role in the proliferation and invasion of prostate cancer (8). Recently, KIF3A was reported to act as a tumor suppressor in NSCLC by suppressing the Wnt/ β -catenin signaling pathway; however, the clinicopathological and prognostic characteristics of patients has not been investigated and presented in enough patients samples (9).

The clinical value of KIF3A and its underlying molecular mechanism in KIF3A are yet to be confirmed. Thus, the present study aimed to identify the role of KIF3A in the carcinogenesis of NSCLC. Taken together, the results provide novel potential therapeutic strategies, suggesting that KIF3A

Correspondence to: Dr Yiqing Qu, Department of Pulmonary and Critical Care Medicine, Qilu Hospital of Shandong University, 107 Wenhuxi Road, Jinan, Shandong 250012, P.R. China
E-mail: quyiqing@sdu.edu.cn

Dr Hong Wang, Department of Thoracic Surgery, Shandong Provincial Qianfoshan Hospital, The First Hospital Affiliated with Shandong First Medical University, 16766 Jingshi Road, Jinan, Shandong 250012, P.R. China
E-mail: hongwang1971@163.com

Key words: non-small cell lung cancer, KIF3A, carcinogenesis, prognosis, IFT57

may act as a potential tumor suppressor in the carcinogenesis of NSCLC.

Materials and methods

Clinical data and tissue specimen. The present study was approved by the Ethics Committee of Qilu Hospital. Patients or their families agreed and provided written informed consent. A total of 163 patients with NSCLC who underwent pneumonectomy at Qilu Hospital between January 2005 and December 2008 were recruited in the present study. Among the 163 patients with NSCLC, 94 were patients with LUAD and 69 were patients with LUSC. The mean age at diagnosis of LUAD was 62.17±9.88 years. The mean age at diagnosis of LUSC was 64.46±8.70 years. All cases were histologically diagnosed as NSCLC (10). Patients who received chemotherapy or radiotherapy prior to surgery were excluded. Patient information, including basic information, pathological type, location of the tumor, TNM stage (according to the 8th edition of the American Joint Committee on Cancer Staging Manual) (11) and prognosis were recorded. Follow-up data were available in all cases, and the longest clinical follow-up period was 121 months. The overall survival (OS) time was defined from the date of surgery to the end of follow-up or the time of death. The clinicopathological characteristics of patients with NSCLC are presented in Table I.

Immunohistochemistry (IHC). Lung tissues were fixed in 4% paraformaldehyde at 4°C for 24 h and imbedded in paraffin. Slices (3 μm) made from 163 paraffin-embedded cancer samples and 157 adjacent normal samples (>5 cm away from the tumor margin) were obtained. Briefly, the tissue sections were incubated at 65°C for 60 min, dewaxed in xylene and subsequently rehydrated in a graded ethanol series. The antigen retrieval process was performed using citrate. Deparaffinized sections were incubated with 3% H₂O₂ for 30 min at 37°C to inhibit endogenous peroxidase activity. Following treatment with 5% bovine serum albumin (BSA) for 30 min at 37°C, tissue sections were incubated with rabbit anti-KIF3A polyclonal antibody in PBS (1:200; cat. no. ab11259; Abcam) overnight at 4°C. The sections were subsequently incubated with the second antibody and streptavidin-biotin complex (SABC) of HRP conjugated anti-Rabbit IgG SABC Kit (cat. no. SA1022; Boster Biological Technology) for 30 min at 37°C. Staining was subsequently performed using the DAB Chromogenic Substrate kit (cat. no. AR1022; Boster Biological Technology) for 1 min and 5 sec, and the slides were counterstained with hematoxylin for 8 min prior to covering with neutral balsam, all at room temperature. The negative control group was processed with PBS instead of the KIF3A antibody, and all other steps were performed as aforementioned. The scorings of the stained sections were calculated as previously described (12).

Cell culture and transfection of small interfering (si)RNA. The human NCI-A549, NCI-H1975 and NCI-H520 NSCLC cell lines, were purchased from The Cell Bank of Type Culture Collection of the Chinese Academy of Sciences and were cultured in RPMI-1640 medium supplemented with 10% FBS at 37°C in a humidified atmosphere with 5% CO₂.

The negative control (NC) siRNA (NC-siRNA) and KIF3A-specific siRNAs (KIF3A-siRNA-1, -2, -3, -4) were constructed by Shanghai GenePharma Co., Ltd. NCI-H520 cells were transfected with siRNAs (100 pmol/per well of 6-well plate) using Lipofectamine[®] 2000 (Thermo Fisher Scientific, Inc.), according to the manufacturer's instructions. After 48 h following transfection, cells were analyzed to determine transfection efficiency using reverse transcription quantitative (RT-qPCR) or used for subsequent experimentation. The sequences of KIF3A-siRNA and the negative control (NC) are presented in Table S1.

RT-qPCR. Total RNA was extracted from KIF3A-siRNA or NC-siRNA transfected cells using TRIzol[®] (Invitrogen; Thermo Fisher Scientific, Inc.) according to the manufacturer's instructions, and the purity and concentration of RNA were assessed using a NanoDrop spectrophotometer (Thermo Fisher Scientific, Inc.). Reverse transcription of the RNA was performed using Moloney Murine Leukemia Virus Reverse Transcriptase (Ambion; Thermo Fisher Scientific, Inc.) and a mixture of anchored Oligo(-dT) (Sangon Biotech Co., Ltd.) and dNTPs (Thermo Fisher Scientific, Inc.). The reaction conditions were as follows: 37°C for 50 min, 70°C for 15 min, 4°C for 5 min. The qPCR (SYBR-Green I) was subsequently performed using UltraSYBR Mixture (CoMin Biosciences) according to the manufacturer's instructions. The following thermocycling conditions were used for qPCR: Initial denaturation at 95°C for 5 min; 40 (two-step) cycles at 95°C for 10 sec and 60°C for 35 sec. Relative expression levels were calculated using the 2^{-ΔΔC_q} method and normalized to the internal reference gene β-actin (13). The following primer sequences were used for qPCR: KIF3A forward, 5'-AGGAGAGTCTGCGTCAGTCT-3' and reverse, 5'-TTTCAGGCTTTGCAGAACGC-3'; IFT57 forward, 5'-ATGGCGGAGTAAGTGAACGG-3' and reverse, 5'-ATCTTCACCAAAGGAGTGCCG-3'; and β-actin forward, 5'-CTCTTCCAGCCTTCCTTCCT-3' and reverse, 5'-AGCACTGTGTTGGCGTACAG-3'.

Cell counting Kit-8 (CCK-8) assay. The proliferative ability of transfected cells was assessed using a CCK-8 assay (Beyotime Institute of Biotechnology). At 48 h following transfection, cells were seeded into 96-well plates, at a density of 2×10³ cells/well and cultured for 24 h. CCK-8 reagent (10 μl) was added into each well and the plates were incubated for 2 h at 37°C. Cell proliferation was measured every 24 h, at 450 nm using a microplate reader (Bio-Rad Laboratories, Inc.). All experiments were performed in triplicate.

Colony formation assay. Cells were seeded into 35 mm dishes, at a density of 500 cells/well and cultured at 37°C with 5% CO₂ for 14 days, 48 h following transfection. Cells were fixed with 4% paraformaldehyde for 30 min at 4°C and subsequently stained with 0.1% crystal violet for 30 min at room temperature. The size and number of the cell colonies was recorded. All experiments were performed in triplicate.

Flow cytometric analysis of apoptosis. Cell apoptosis was determined using the Annexin V-fluorescein isothiocyanate (FITC)/propidium iodide (PI) Apoptosis Detection kit (KeyGEN BioTECH). Cells were collected using trypsin

Table I. Clinicopathological characteristics of patients with non-small cell lung cancer.

Variables	LUAD, n (%)	LUSC, n (%)
Total number of patients	94 (100)	69 (100)
Sex		
Male	51 (54.3)	43 (62.3)
Female	43 (45.7)	26 (37.7)
Age at diagnosis, years		
≤60	43 (45.7)	20 (29.0)
>60	51 (54.3)	49 (71.0)
Smoking status		
Non-smoking	39 (41.5)	28 (40.6)
Smoking	55 (58.5)	41 (59.4)
Primary tumor location		
Left lung	40 (42.6)	27 (39.1)
Right lung	54 (57.4)	42 (60.9)
Differentiation grade		
High and middle	69 (73.4)	51 (73.9)
Low	25 (26.6)	18 (26.1)
Primary tumor size		
T1+T2	71 (75.5)	50 (72.5)
T3+T4	23 (24.5)	19 (27.5)
Lymph node metastasis		
N0	42 (44.7)	42 (60.9)
N1-3	52 (55.3)	27 (39.1)
Stage grouping with TNM		
Stage I + II	55 (58.5)	53 (76.8)
Stage III + IV	39 (41.5)	16 (23.2)

LUAD, lung adenocarcinoma; LUSC, lung squamous cell carcinoma.

without EDTA and washed three times with cold PBS, 48 h following transfection. Cells were resuspended in 400 μ l Annexin V-Binding buffer, at a density of 1×10^6 cells/ml, and incubated with 5 μ l Annexin V-FITC and 10 μ l PI for 5 and 15 min, respectively, at 37°C in the dark. Apoptotic cells were subsequently analyzed using FlowJo software (version 10; Excyte). All experiments were performed in triplicate.

Wound healing assay. The cells were seeded into 6-well plates (1×10^6 cells/well) and cultured until they reached full confluency, 48 h following transfection. Adherent cells were aspirated using a micropipette tip to create ~1-mm cell-free zones. The cells were washed three times with PBS and the plate was cultured in medium with 1% FBS at 37°C with 5% CO₂. Images were captured with an inverted microscope (Olympu Corporation; magnification, x40) at 0 and 24 h during incubation. The wound closure rate was calculated. Scratch healing rate=(healing area at 0 h-healing area at 24 h)/healing area at 0 h.

Transwell migration and invasion assay. The cell migratory and invasive abilities were determined using the polycarbonate membranes (8- μ m pore size) of Transwell migration (cat.

no. 3422) and invasion chambers (cat. no. 354480) (both from Corning, Inc.), respectively, 48 h following transfection. The migration and invasion assays were performed as previously described (12).

Protein extraction and western blot analysis. For protein extraction, cells were lysed in RIPA buffer (Beyotime Biotechnology) supplemented with protease inhibitors (Beyotime Institute of Biotechnology). After incubation on ice for 15 min, the lysate was centrifuged at 13,800 x g for 15 min at 4°C, and the supernatant was collected. Protein concentration was calculated using a BCA Protein Assay kit (cat. no. P0010S; Beyotime Institute of Biotechnology). Protein extracts were separated using 10% SDS-PAGE and transferred onto polyvinylidene fluoride membranes. After blocking with 5% skimmed milk and incubated with rabbit polyclonal anti-intraflagellar transport 57 (IFT57) (1:1,000 dilution; cat. no. ab5205; Abcam) and rabbit anti-GAPDH (1:1,000 dilution; cat. no. 2118; Cell Signaling Technology, Inc.) overnight at 4°C, the membranes were incubated with anti-rabbit IgG (1:5,000 dilution; cat. no. AQ132P; EMD Millipore). After washing with TBS-Tween-20, the protein bands were detected using an enhanced chemiluminescence western blotting substrate kit (Thermo Fisher Scientific, Inc.). Relative protein levels were quantified by scanning densitometry using ImageJ software (version 1.4.3; National Institutes of Health).

Bioinformatics analysis. The Kaplan-Meier (K-M) Plotter database was used to investigate the association between KIF3A mRNA expression levels with OS time, first progression (FP) and post-progression survival (PPS) (<http://kmplot.com/analysis/index.php?p=service&cancer=lung>) (14). FP is the time to first progression, and PPS is the OS time minus the time to disease progression (15). The association between IFT57 mRNA expression levels and OS time was also assessed. Sources for the K-M Plotter database include Gene Expression Omnibus (GEO), European Genome-phenome Archive (EGA), and The Cancer Genome Atlas (TCGA). The collection and sort of data, quality check, normalization and survival calculation were executed by the database. The median value of mRNA expression was chosen as the cut off value. Samples with mRNA expression values higher than the median value were included in the high expression group, while values below the median were included in the low expression group. The classified cohorts were compared using K-M survival plots, and hazard ratios (HR), 95% confidence intervals (CIs) and log-rank P-values were recorded.

The correlation between KIF3A expression and survival in LUAD and LUSC was also analyzed using the PrognoScan database (16). PrognoScan searches for associations between gene expression and patient prognosis, including OS and relapse-free survival (RFS) time, across a large collection of publicly available cancer microarray datasets. The threshold was adjusted to a Cox P<0.05.

A protein-protein interaction (PPI) network of KIF3A was constructed using the Search Tool for the Retrieval of Interacting Genes (STRING) database (17). The differential mRNA expression levels of KIF3B, KIF3C, IFT57, IFT52, IFT20, IFT172, DYNC2H1, IFT88, KIFAP3, and DCTN1 between LUAD and adjacent normal tissues, and LUSC and

Table II. Association of KIF3A protein expression level in tumor tissues with the clinicopathological characteristics in patients with lung adenocarcinoma (n=94).

Clinicopathological characteristics	KIF3A expression			Pearson's χ^2	P-value
	Number	Low, n (%)	High, n (%)		
Sex					
Male	51	27 (52.9)	24 (47.1)	0.386	0.535
Female	43	20 (46.5)	23 (53.5)		
Age at diagnosis, years					
≤ 60	43	25 (58.1)	18 (41.9)	2.1	0.147
> 60	51	22 (43.1)	29 (56.9)		
Smoking status					
No smoking	39	18 (46.2)	21 (53.8)	0.004	0.947
Smoking	55	25 (45.5)	30 (54.5)		
Primary tumor location					
Left lung	40	17 (42.5)	23 (57.5)	1.567	0.211
Right lung	54	30 (55.6)	24 (44.4)		
Differentiation grade					
High and middle	69	39 (56.5)	30 (43.5)	4.414	0.036 ^a
Low	25	8 (32.0)	17 (68.0)		
Primary tumor size					
T1+T2	71	32 (45.1)	39 (54.9)	2.821	0.093
T3+T4	23	15 (65.2)	8 (34.8)		
Lymph node metastasis					
N0	42	20 (47.6)	22 (52.4)	1.172	0.678
N1-3	52	27 (51.9)	25 (48.1)		
Stage grouping with TNM					
Stage I + II	55	22 (40.0)	33 (60.0)	5.303	0.021 ^a
Stage III + IV	39	25 (64.1)	14 (35.9)		

^aP<0.05. KIF3A, kinesin family member 3A.

adjacent normal tissues, were validated using the GEPIA online analysis tool (18). mRNA expression levels were determined using the following settings: 'Multiple gene comparison'; 'tissue order=LUAD and LUSC'; 'log scale=yes'; and 'match TCGA normal data'. The association between *KIF3A* and *IFT57* mRNA expression levels in NSCLC was also assessed using GEPIA, using the following settings: 'Correlation'; 'gene A=KIF3A'; 'gene B=IFT57'; 'Correlation coefficient=Spearman' and 'datasets=TCGA tumor'.

IFT57 mRNA expression level in 291 unique datasets of common human cancers, including bladder cancer, breast cancer, cervical cancer and lung cancer, was determined using the Oncomine datasets (www.oncomine.org). The settings were as follows: 'Gene, KIF3A'; 'analysis type: Cancer vs. normal analysis'; 'cancer type: Lung cancer'; 'data type: mRNA'; 'sample type: Clinical specimen'; 'threshold (P-value): 0.0001'; 'threshold (fold change): 2' and 'threshold (gene rank): Top 10%'.

RNA-Sequencing (RNA-Seq) microarray gene expression levels of *KIF3A* and *IFT57* in NSCLC cell lines were determined using the Cancer Cell Line Encyclopedia (CCLE) (19). Robust Multi-array Average (RMA) normalization was

performed (20). The correlation between *KIF3A* and *IFT57* expression levels was determined using the Pearson's rank correlation test.

Statistical analysis. The statistical analyses were performed using SPSS v21.0 software (IBM Corp.) and GraphPad v6.0 (GraphPad Software, Inc.). Data are presented as the mean \pm SD. An unpaired Student's t-test was used to compare data from the cell experiments. A Kolmogorov-Smirnov test was used to analyze the normal distribution of variables. The mRNA levels of *KIF3A* in multiple NSCLC cell lines were analyzed using one-way ANOVA and Tukey's post hoc test. The mRNA levels of *KIF3A* in H520 cells transfected with NC-siRNA and *KIF3A*-siRNA-1 to 4 were compared using one-way ANOVA and Dunnett's post hoc test. The IHC scores of NSCLC and adjacent normal tissues were compared using a paired Student's t-test. The Mann-Whitney U test was performed to compare differences between two groups when quantitative variables were not normally distributed. A χ^2 test was used to compare clinical variables between groups. The K-M method and log-rank test were used to calculate the OS rate. Univariate Cox regression proportional hazards model

Table III. Association of KIF3A mRNA expression level in tumor tissues with the clinicopathological characteristics in patients with lung squamous cell carcinoma (n=69).

Clinicopathological characteristic	KIF3A expression			Pearson's χ^2	P-value
	Number	Low, n (%)	High, n (%)		
Gender					
Male	43	22 (51.2)	21 (48.8)	0.163	0.687
Female	26	12 (46.2)	14 (53.8)		
Age at diagnosis, years					
≤60	20	11 (55.0)	9 (45.0)	0.369	0.543
>60	49	23 (46.9)	26 (53.1)		
Smoking status					
Non-smoking	28	9 (32.1)	19 (67.9)	5.534	0.019 ^a
Smoking	41	25 (61.0)	16 (39.0)		
Primary tumor location					
Left lung	27	13 (48.1)	14 (51.9)	0.023	0.881
Right lung	42	21 (50.0)	21 (50.0)		
Differentiation grade					
High and middle	51	25 (49.0)	26 (51.0)	0.005	0.943
Low	18	9 (50.0)	9 (50.0)		
Primary tumor size					
T1+T2	50	24 (48.0)	26 (52.0)	0.118	0.731
T3+T4	19	10 (52.6)	9 (47.4)		
Lymph node metastasis					
N0	43	17 (39.5)	26 (60.5)	4.332	0.037 ^a
N1-3	26	17 (65.4)	9 (34.6)		
Stage Grouping with TNM					
Stage I + II	53	28 (52.8)	25 (47.2)	1.156	0.282
Stage III + IV	16	6 (37.5)	10 (62.5)		

^aP<0.05. KIF3A, kinesin family member 3A.

was performed to calculate the effect of variables on OS. Variables with P<0.1 in the univariate analysis were included in the multivariate analysis. P<0.05 was considered to indicate a statistically significant difference.

Results

Low KIF3A protein expression in clinical NSCLC and its association with the clinicopathological characteristics. The expression and subcellular localization of the KIF3A protein in clinical NSCLC tissues (n=163) and adjacent normal tissues (n=157) were determined using IHC analysis (Fig. 1A-F). The results showed that the KIF3A protein was predominantly stained in the cellular membrane and the cytoplasm of NSCLC cells. KIF3A protein expression level in the tumor tissues of patients with LUAD (n=94) and LUSC (n=69) was significantly lower compared with that in the respective adjacent normal tissues (P<0.01 and P<0.05, respectively; Fig. 1G). Furthermore, KIF3A protein expression was lower in patients with LUAD compared with that in patients with LUSC (P<0.001; Fig. 1G).

The association between KIF3A protein expression level and the clinicopathological characteristics of patients with LUAD

and LUSC are presented in Tables II and III, respectively. In patients with LUAD, low KIF3A expression was significantly associated with TNM stage (P=0.021), whereas high KIF3A expression was significantly associated with tumor differentiation grade (P=0.036). Conversely, in patients with LUSC, low KIF3A expression was significantly associated with smoking status (P=0.019) and lymph node metastasis (P=0.037).

Univariate Cox regression analysis demonstrated that lymph node metastasis (HR, 2.427; 95% CI, 1.478-3.958; P<0.001) and TNM stage (HR, 2.843; 95% CI, 1.748-4.624; P<0.001) were significantly negative prognostic factors for OS time in patients with LUAD. Multivariate Cox regression analysis demonstrated that TNM stage was an independent prognosis factor for OS time (HR, 2.148; 95% CI, 1.167-3.952; P=0.014) (Table IV).

In patients with LUSC, TNM stage (HR, 2.448; 95% CI, 1.170-5.122; P=0.017) was also demonstrated to be a negative prognostic factor for OS time following univariate Cox regression analysis. However, no significant difference between OS time and KIF3A protein expression level were observed following multivariate Cox regression (Table IV). And there was no significant association between OS time

Table IV. Univariate and multivariate analyses of prognostic factors of overall survival in patients with LUSC and LUAD.

A, Overall survival in patients with LUAD						
Clinicopathological characteristics	Univariate analysis			Multivariate analysis		
	HR	P-value	95% CI	HR	P-value	95% CI
KIF3A expression (low vs. high)	1.007	0.976	0.629-1.612			
Sex (male vs. female)	0.733	0.198	0.457-1.176			
Age at diagnosis (≤ 60 vs. >60 years)	1.011	0.962	0.632-1.619			
Smoking status (non-smoking vs. smoking)	1.598	0.774	1.023-1.984			
Primary tumor location (left lung vs. right lung)	0.99	0.967	0.614-1.595			
Differentiation grade (high and middle vs. low)	0.982	0.947	0.568-1.696			
Primary tumor size (T1+T2 vs. T3+T4)	1.424	0.191	0.838-2.419			
Lymph node metastasis (N0 vs. N1-3)	2.427	$<0.001^a$	1.478-3.958	1.569	0.158	0.840-2.931
Stage grouping with TNM (I + II vs. III + IV)	2.843	$<0.001^a$	1.748-4.624	2.148	0.014 ^b	1.167-3.952

B, Overall survival in patients with LUSC

B, Overall survival in patients with LUSC						
Clinicopathological characteristics	Univariate analysis			Multivariate analysis		
	HR	P-value	95% CI	HR	P-value	95% CI
KIF3A expression (low vs. high)	1.692	0.143	0.837-3.420			
Sex (male vs. female)	1.024	0.946	0.512-2.048			
Age at diagnosis (≤ 60 vs. >60 years)	2.041	0.114	0.842-4.948			
Smoking status (non-smoking vs. smoking)	0.625	0.203	0.303-1.289			
Primary tumor location (left lung vs. right lung)	0.745	0.402	0.373-1.485			
Differentiation grade (high and middle vs. low)	1.477	0.305	0.701-3.111			
Primary tumor size (T1+T2 vs. T3+T4)	1.616	0.194	0.783-3.336			
Lymph node metastasis (N0 vs. N1-3)	1.544	0.216	0.776-3.070			
Stage grouping with TNM (I + II vs. III + IV)	2.448	0.017 ^b	1.170-5.122			

^aP<0.001. ^bP<0.05. LUAD, lung adenocarcinoma; LUSC, lung squamous cell carcinoma; HR, hazard ratio; CI, confidence interval; KIF3A, kinesin family member 3A.

and KIF3A protein expression in LUAD and LUSC using K-M survival analyses (both P>0.05; Fig. S1A and B, respectively).

Low KIF3A expression predicts poor prognosis in K-M Plotter and the PrognScan database. The prognostic value of KIF3A mRNA expression on NSCLC was further investigated using the K-M Plotter database. Low KIF3A expression was significantly associated with adverse OS time (HR, 0.6; P<0.001; Fig. 1H) in 1,144 patients with NSCLC. In patients with LUAD (n=672), low KIF3A expression was associated with adverse OS time (HR, 0.45; P<0.001; Fig. 1I). Furthermore, low KIF3A expression was associated with first progression (FP; HR, 0.67; P=0.014; Fig. 1J) and the post-progression survival (PPS; HR, 0.53; P=0.011; Fig. 1K) of patients with LUAD. However, no significant association was observed between KIF3A expression and OS time in patients with LUSC (n=271).

To further validate the prognostic effect of KIF3A, the data was analyzed using a second database PrognScan. Notably,

the results demonstrated that the GSE31210 cohort (21), which included 226 samples of patients with LUAD, showed that low KIF3A expression was significantly associated with poor prognosis (OS HR, 0.13, 95% CI, 0.05 to 0.33, Cox P<0.001; Fig. S2A; RFS HR, 0.19, 95% CI, 0.09 to 0.39, Cox P<0.001; Fig. S2B). There was no prognostic value of KIF3A expression in patients with LUSC (GSE4573 and GSE17710) (22,23).

Prognostic value of KIF3A in patients with NSCLC according to clinicopathological characteristics and treatment, using the K-M Plotter database. The association between KIF3A expression and smoking status, sex, clinical stages, and different chemotherapeutic treatments of patients with NSCLC was determined. As presented in Table V, low KIF3A mRNA expression level was associated with adverse OS time in patients with a smoking history (HR, 0.56; P=0.0068; Fig. S3A) and without a smoking history (HR, 0.15; P<0.001; Fig. S3B). Furthermore, low KIF3A mRNA expression was associated with poor OS time in female (HR, 0.41; P<0.001; Fig. S3C) and male (HR, 0.69;

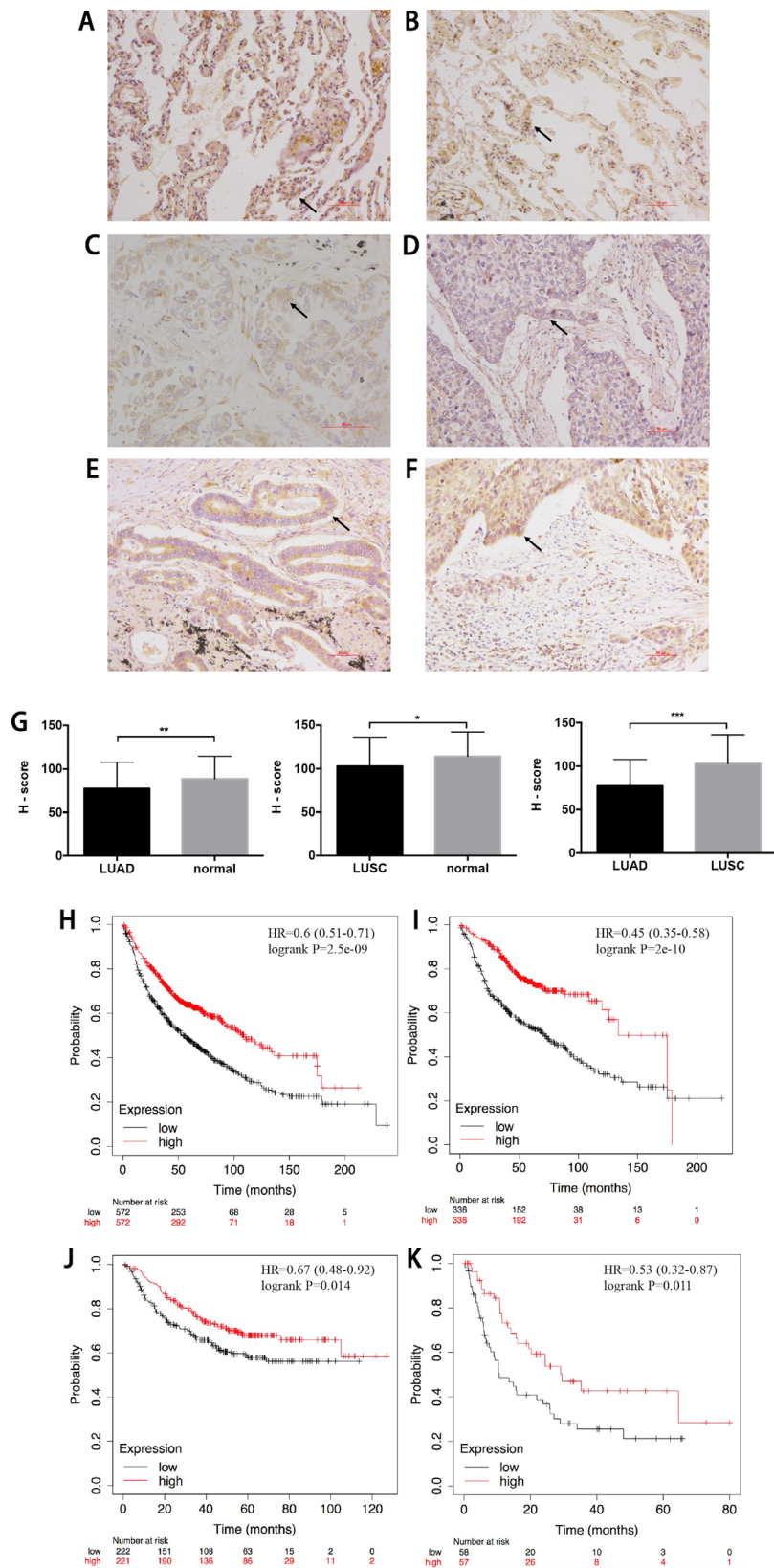


Figure 1. Protein expression level of KIF3A in NSCLC tissues determined using immunohistochemistry and survival analyses. (A) and (B) KIF3A protein expression in the tumor and adjacent normal tissues. (C) Low expression of the KIF3A protein in the adenocarcinoma tissues. (D) Low expression of KIF3A protein in the squamous cell carcinoma tissues. (E) High expression of KIF3A protein in the adenocarcinoma tissues. (F) High expression of KIF3A protein in the squamous cell carcinoma tissues. (scale bar, 50 μ m). (G) Semi-quantitative analyses of the KIF3A protein expression level in the NSCLC and adjacent normal tissues. * $P < 0.05$, ** $P < 0.01$, *** $P < 0.001$. Paired Student's t-test was used for the comparison of NSCLC with the adjacent normal tissue, while Mann-Whitney U test was used for the comparison of LUAD with LUSC. (H) The OS time was shorter in the patients with low mRNA expression level of KIF3A compared with those with a high expression level in all of the patients with NSCLC from the K-M Plotter database (K-M method with log-rank test). The low mRNA expression level of KIF3A was associated with poor (I) OS, (J) FP and (K) PPS in patients with LUAD from the K-M Plotter database (K-M method with log-rank test). K-M, Kaplan-Meier; OS, overall survival; FP, first progression; PPS, post-progression survival; LUAD, lung adenocarcinoma; LUSC, lung squamous cell carcinoma; NSCLC, non-small cell lung cancer; KIF3A, kinesin family member 3A; H-score, IHC scores.

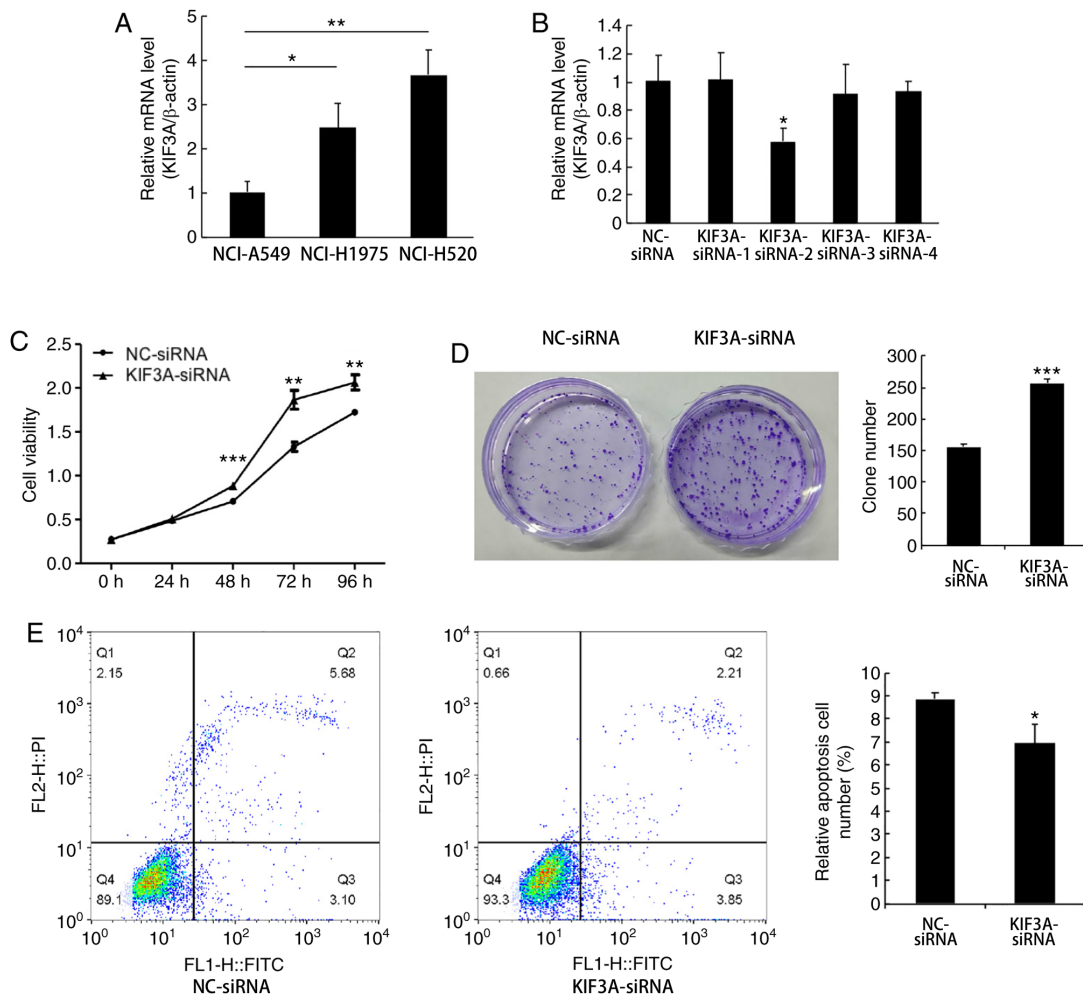


Figure 2. mRNA expression level of KIF3A in the NSCLC cell lines and KIF3A knockdown promotes proliferation. (A) The mRNA expression levels of KIF3A in three NSCLC cell lines A549, H1975 and H520. The data was analyzed using one-way ANOVA following by Tukey's post hoc test. (B) The mRNA expression level of *KIF3A* in H520 cells transfected with NC-siRNA or KIF3A-siRNA-1 to 4. The data was analyzed using one-way ANOVA followed by Dunnett's post hoc test, compared with that in the control group. (C) The cell proliferation ability was significantly enhanced in the KIF3A-siRNA group compared with that in the NC-siRNA group using a Cell Counting Kit-8 assay (Student's t-test). (D) The KIF3A-siRNA transfected cells formed larger and more colonies compared with that in the siNC cells in the colony formation assay (Student's t-test). (E) Cell apoptosis was inhibited in cells transfected with KIF3A-siRNA (Student's t-test). * $P < 0.05$, ** $P < 0.01$, *** $P < 0.001$. si, short inhibiting, NC, negative control; KIF3A, kinesin family member 3A; NSCLC, non-small cell lung cancer.

$P < 0.001$; Fig. S3D). For patients in clinical stage I (HR, 0.43; $P < 0.001$; Fig. S3E) and T1 stage (HR, 0.65; $P = 0.0302$; Fig. S3F), low KIF3A mRNA expression was associated with adverse OS. In addition, low KIF3A expression was significantly associated with poor OS time in surgically successful patients (HR=0.21; $P < 0.001$; Fig. S3G). However, KIF3A failed to exhibit prognostic value in patients with stage II-IV, T2-3, lymph node metastasis and chemotherapeutic treatment history.

KIF3A expression in the NSCLC cell lines. KIF3A mRNA expression was determined in 3 NSCLC cell lines (NCI-A549, NCI-H1975 and NCI-H520). The results demonstrated that the relative mRNA expression levels of KIF3A in NCI-H1975 and NCI-H520 cells were higher compared with that in the NCI-A549 cells (NCI-A549 vs. NCI-H1975, $P < 0.05$; NCI-A549 vs. NCI-H520, $P < 0.01$; Fig. 2A). Therefore, the following functional experiments were performed using the NCI-H520 cell line.

RNA interference efficiently suppresses KIF3A expression in NCI-H520 cells. The NCI-H520 cells were divided into

two groups, the NC group (NC-siRNA transfected cells) and the siRNA group (KIF3A-siRNA transfected cells). The knockdown efficiency of four siRNAs was determined using RT-qPCR. The results demonstrated that the KIF3A mRNA expression level was significantly downregulated by KIF3A-siRNA-2, compared with that in the NC-siRNA groups, and was the most effective (42%; $P < 0.05$; Fig. 2B).

KIF3A knockdown promotes proliferation and inhibits apoptosis of NCI-H520 cells. To investigate the effect of KIF3A downregulation on cell proliferation, the CCK-8 assay was performed in transfected NCI-H520 cells. The results demonstrated that the proliferative ability was enhanced in the KIF3A-siRNA group compared with that in the NC-siRNA group ($P < 0.01$; Fig. 2C). The colony formation assay demonstrated that cells in the KIF3A-siRNA group formed significantly larger and more colonies compared with that in the NC-siRNA group ($P < 0.001$; Fig. 2D).

Cell apoptosis was investigated using flow cytometric analysis, and Annexin V-FITC/PI double staining. The

Table V. Prognostic value of kinesin family member 3A expression level in patients with non-small cell lung cancer according to clinicopathological characteristics and treatment using the K-M Plotter database.

Clinicopathological characteristics	Number	Cutoff value	Median survival, months		K-M		
			Low expression cohort	High expression cohort	HR	P-value	95% CI
Cancer type							
LUAD	672	376	71.27	133.57	0.45	<0.001	0.35-0.58
LUSC	271	212	63	51.53	1.06	0.7246	0.78-1.44
Smoking status							
Smoked	300	367	35	48	0.56	0.0068	0.37-0.86
Never smoked	141	643	/	/	0.15	<0.001	0.05-0.45
Sex							
Female	374	393	23	69.93	0.41	<0.001	0.28-0.59
Male	659	304	52	90	0.69	<0.001	0.56-0.85
Stage							
I	449	390	33.37	72.33	0.43	<0.001	0.3-0.6
II	161	350	57	88.7	0.66	0.075	0.42-1.05
III	44	312	14.93	26.09	0.79	0.5156	0.4-1.59
IV	4	/	/	/	/	/	/
Primary tumor size							
T1	224	243	71	175	0.65	0.0302	0.43-0.96
T2	190	211	76	48	1.45	0.0591	0.98-2.13
T3	29	270	35	13	1.55	0.2917	0.68-3.52
T4	23	397	9	28	0.57	0.2004	0.23-1.37
Lymph node metastasis							
N0	324	235	107	91	1.07	0.6735	0.78-1.46
N1	102	189	60	36	0.93	0.7677	0.56-1.53
N2	32	402	21	11	1.3	0.4806	0.63-2.71
Metastasis							
M0	462	239	70	72	1.1	0.45	0.86-1.41
M1	10	/	/	/	/	/	/
Treatment							
Surgery success ^a	204	664	/	/	0.21	<0.001	0.09-0.52
Chemotherapy							
No	22	505	26.09	43.07	0.94	0.9387	0.19-4.69
Yes	34	430	32.95	36.24	1.44	0.5354	0.45-4.62

^aOnly surgical margins negative. LUAD, lung adenocarcinoma; LUSC, lung squamous cell carcinoma; HR, hazard ratio; CI, confidence interval; K-M, Kaplan-Meier; /, the data not shown in the database.

results demonstrated that the apoptotic rate of transfected NCI-H520 cells was significantly downregulated in the KIF3A-siRNA group compared with that in the NC-siRNA group (P<0.05; Fig. 2E).

KIF3A knockdown promotes metastasis and invasion of the NCI-H520 cells. The wound healing assay was performed using the NCI-H520 cells and the results demonstrated an enhanced migratory ability in KIF3A-siRNA cells compared with that in the NC-siRNA group (P<0.001; Fig. 3A). The Transwell migration and invasion assays demonstrated enhanced migratory and invasive abilities in the

KIF3A-siRNA group (P<0.01 and P<0.001; Fig. 3B and C, respectively).

KIF3A expression correlates with IFT57 expression in patients with NSCLC and NSCLC cell lines. To identify the proteins interacting with KIF3A, a PPI network of KIF3A was constructed using the STRING database (Fig. 4A). The mRNA expression levels of these 11 molecules in the NSCLC samples were assessed using GEPIA (Fig. 4B). The density of color in each block of Fig. 4B represents the median expression value of the molecule in tissues. The results demonstrated that only IFT57 was significantly expressed at low levels in

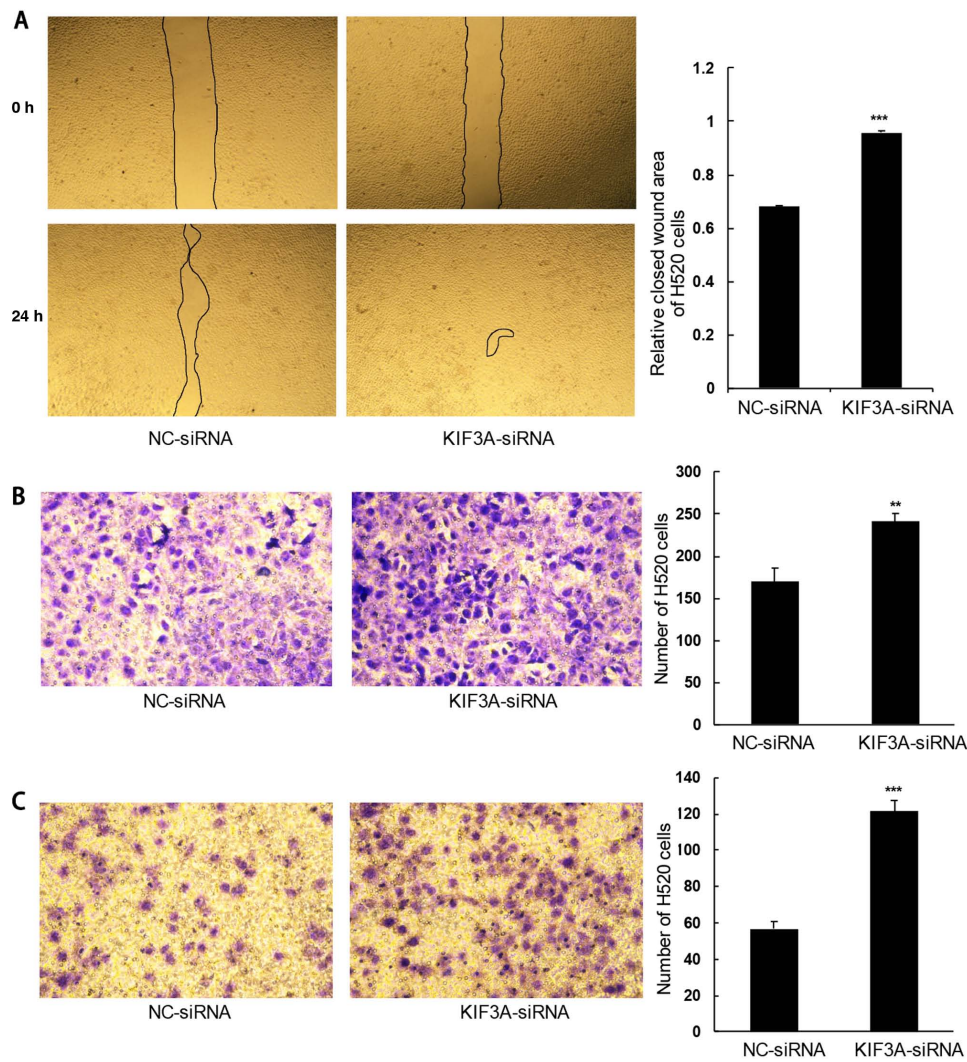


Figure 3. Migration and invasion abilities were increased following KIF3A knockdown in the H520 cells. (A) The migration ability was enhanced in cells transfected with KIF3A-siRNA compared with that in cells transfected with siNC using wound healing assay. The (B) migration and (C) invasion abilities were increased in cells transfected with KIF3A-siRNA compared with that in cells transfected with siNC using Transwell migration and invasion assays. ** $P < 0.01$, *** $P < 0.001$. The data was compared using a Student's t-test. si, short inhibiting; NC, negative control; KIF3A, kinesin family member 3A.

both LUAD and LUSC samples compared with that in the adjacent normal samples (Fig. 4C). Thus, IFT57 was selected for further analyses.

IFT57 mRNA expression level in 291 datasets was assessed using the Oncomine database, comparing expression between tumor and adjacent normal samples (Fig. 4D). A total of 22 datasets exhibited statistically significant differences in IFT57 expression between tumor and adjacent normal samples. Among these 22 datasets, 5 studies demonstrated increased IFT57 expression, while 17 studies demonstrated decreased IFT57 expression in the cancer groups. Among the common malignant tumors, 4 studies had low expression in colorectal cancer, 3 studies had low expression in lymphoma and 2 studies had high expression in myeloma. There were 6 studies with low expression and no studies with high expression of IFT57 in lung cancer.

Correlation analysis of the clinical NSCLC samples from TCGA was performed, and the results demonstrated a significantly positive correlation between KIF3A and IFT57 expression in LUAD and LUSC samples (both $P < 0.001$; $r = 0.2$ and $r = 0.3$, respectively; Spearman's rank correlation

test; Fig. 5A). To further validate this result, correlation analysis between KIF3A and IFT57 mRNA expression was performed in multiple NSCLC cell lines using CCLE, and RNA-Seq. Similarly, the results demonstrated a significantly positive correlation between KIF3A and IFT57 mRNA expression levels ($P < 0.001$; $r = 0.311$; Spearman's rank correlation test; Fig. 5B).

Furthermore, the IFT57 mRNA and protein expression level was determined at 48 h following transfection with siRNA in the H520 cells and the results showed that the mRNA and protein expression levels of IFT57 were downregulated in KIF3A-siRNA cells compared with that in the siNC cells ($P < 0.001$; Fig. 5C).

Low IFT57 expression indicates poor prognosis in NSCLC.

The association between IFT57 mRNA expression level and prognosis was determined using the K-M Plotter database and the results demonstrated that low IFT57 mRNA expression in NSCLC was associated with adverse OS time (HR, 0.67; $P = 0.014$; Fig. 5D). A similar result was also found in patients with LUAD (HR, 0.55; $P = 0.011$; Fig. 5E). However, no

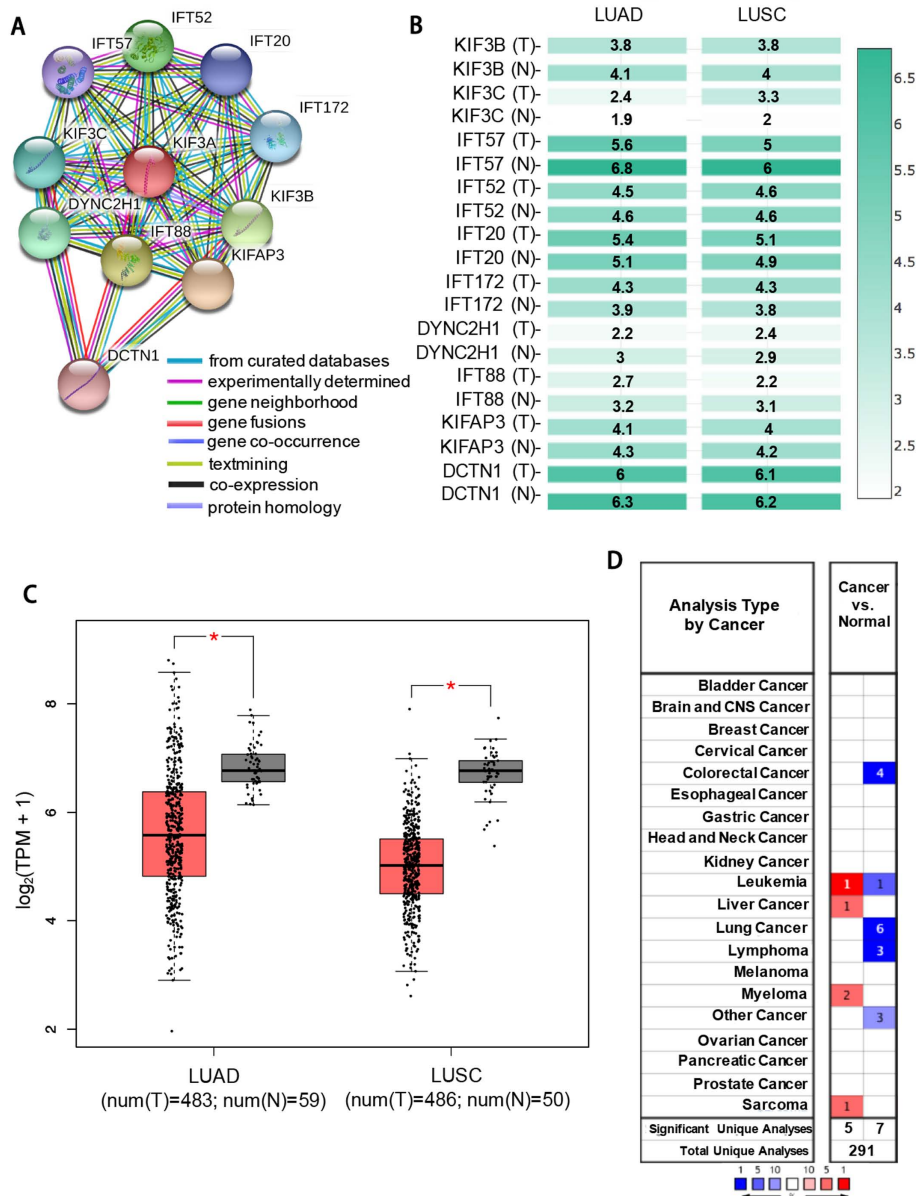


Figure 4. IFT57 interacts with KIF3A and the mRNA expression level is decreased in NSCLC. (A) Protein-protein interaction network of KIF3A using the Search Tool for the Retrieval of Interacting Genes database. Edges represent protein-protein associations. (B) The mRNA expression level of 11 interacting molecules in LUAD and LUSC samples from The Cancer Genome Atlas. The density of color in each block represents the median expression value of the molecule in tissues. (C) IFT57 expression was significantly lower in both LUAD and LUSC samples compared with that in their respective normal samples. (D) The mRNA expression level of IFT57 in 291 different cancer studies using the Oncomine database. The number in the colored block represents the number of studies meeting thresholds. The color is determined by the gene rank. The intensity of red (overexpression) or blue (under expression) indicates the degree of gene expression. *P<0.05. T, tumor; N, normal; LUAD, lung adenocarcinoma; LUSC, lung squamous cell carcinoma; TPM, transcripts per million; KIF3A, kinesin family member 3A; IFT57, intraflagellar transport 57.

significant association was observed between IFT57 mRNA expression and OS time in patients with LUSC.

Discussion

Progress has been made in the diagnosis and treatment of NSCLC; however, the survival outcome of patients remains poor due to metastasis and occurrence (2). Thus, there is an urgent requirement to further investigate the molecular mechanisms underlying NSCLC occurrence and metastasis. The results of the present study demonstrated that KIF3A protein expression level was decreased in patients with NSCLC. Furthermore, KIF3A knockdown increased the proliferative,

invasive and metastatic abilities, and inhibited apoptosis of NSCLC cells *in vitro*. KIF3A mRNA expression level was positively correlated with IFT57 mRNA expression level in NSCLC. In addition, poor survival of patients with NSCLC was associated with low IFT57 expression. Taken together, these results suggested that KIF3A may act as a potential tumor suppressor in NSCLC.

Low KIF3A protein expression level was associated with TNM stage in LUAD and lymph node metastasis in LUSC. Based on the analyses using the K-M plotter database, low KIF3A mRNA expression level was associated with a low OS time in patients with NSCLC. In addition, low KIF3A mRNA expression level was an independent risk factor and was associated

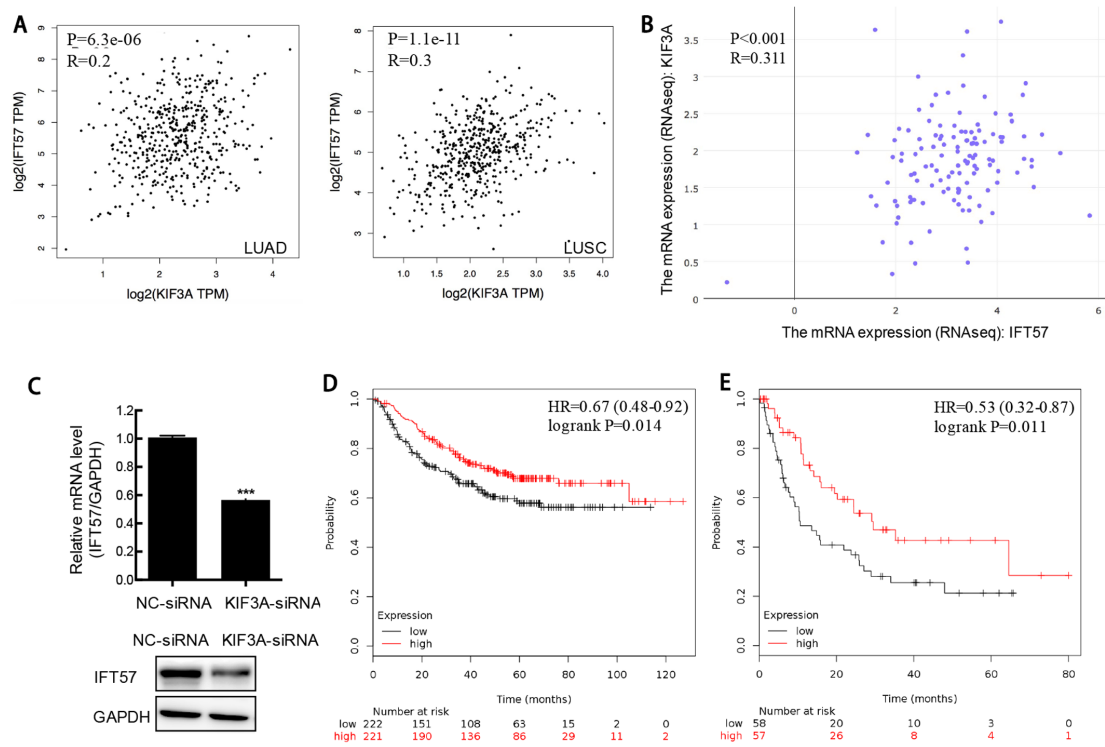


Figure 5. IFT57 mRNA expression level positively correlates with KIF3A mRNA expression level and prognosis analysis of IFT57. (A) The positive correlation between KIF3A and IFT57 mRNA expression levels in LUAD and LUSC samples from The Cancer Genome Atlas database. (B) KIF3A mRNA expression level was positively correlated with IFT57 mRNA expression level in the NSCLC cell lines. (C) The mRNA and protein expression levels of IFT57 were decreased following KIF3A knockdown in the H520 cell line. The data was analyzed using a Student's t-test. *** $P<0.001$. Poor OS time was associated with low expression level of IFT57 in (D) patients with NSCLC and (E) patients with LUAD. LUAD, lung adenocarcinoma; LUSC, lung squamous cell carcinoma; KIF3A, kinesin family member 3A; IFT57, intraflagellar transport 57; OS, overall survival; seq, sequencing; TPM, transcripts per million.

with poor prognosis in LUAD using PrognScan. Furthermore, the same outcome was exhibited in patients with NSCLC, with clinical stage I and T1 grade, indicating the prognostic value of KIF3A in patients with early-stage NSCLC. The survival time of patients with NSCLC usually varies, even in patients with similar clinical stages and those who receive similar treatment strategies (24,25). Further studies are required to identify novel prognostic biomarkers. Previously, potential factors with promising prognostic value have been reported in patients with NSCLC, like increased infiltration of regulatory T cells into core tumor regions and tripartite motif-containing 37 (26,27). The results of the present study demonstrated that low mRNA and protein expression level of KIF3A may be an effective diagnostic and prognostic marker of NSCLC.

KIF3 is a heterotrimeric complex comprising of KIF3A, KIF3B and kinesin-associated protein 3 (KAP3) (28). Previous studies reported the function of KIF3A in different types of lung diseases. KIF3A mRNA and protein expression was decreased in asthma, while KIF3A knockdown promoted the apoptosis of bronchial epithelia (29). Another study demonstrated that the defective KIF3A-mediated loss of cilia in human type II alveolar epithelial cell lines disrupts the Sonic hedgehog signaling pathway (30). In addition, it has been reported that KIF3A binds to β -arrestin and suppresses the Wnt/ β -catenin signaling pathway independently of primary cilia in lung cancer (9). The results of our study demonstrated that KIF3A was involved in the proliferation and metastasis of NSCLC, whereby KIF3A knockdown resulted in inhibition of cell proliferation, migration and invasion *in vitro*.

The potential molecular mechanisms underlying KIF3A in NSCLC were also investigated. IFT57 was demonstrated to interact with KIF3A, and IFT57 mRNA expression level was significantly reduced in NSCLC. Furthermore, KIF3A mRNA expression was positively correlated with IFT57 mRNA expression level in the clinical NSCLC samples and NSCLC cell lines. In addition, the mRNA and protein expression levels of IFT57 were decreased following KIF3A knockdown in the H520 cell line. The results demonstrated that low IFT57 mRNA expression level was associated with adverse survival of patients with NSCLC. However, to the best of our knowledge, the clinical significance of IFT57 and its potential function have not been investigated in any cancer studies. Previous studies have demonstrated that IFT, containing IFT-A and IFT-B complexes, was essential for the formation and maintenance of cilia (31-33). The bidirectional transportation of ciliary proteins along the axonemal microtubules and ciliary entry and exit are regulated by IFT molecules, including IFT-A and IFT-B (31-33). A recent study reported a three-to-four protein interaction, including the kinesin-II trimer KIF3A-KIF3B-KAP3 and the IFT-B-connecting tetramer IFT38-IFT52-IFT57-IFT88 (34). However, to the best of our knowledge, the interaction between KIF3A and IFT57 has not yet been reported. Collectively, the results of the present study suggested that KIF3A may interact with IFT57 in NSCLC, and IFT57 may also be a potential diagnostic and prognostic biomarker for NSCLC.

The present study is not without limitations. Firstly, large-scale prospective studies are required to further assess

the diagnostic and prognostic values of KIF3A and IFT57 in NSCLC. The results from the public databases were not verified using clinical samples. These conflicting results may be due to different sample sources and sample sizes. Secondly, the molecular mechanism underlying the interaction between KIF3A and IFT57 in NSCLC required verification in future studies.

In conclusion, the results of the present study demonstrated that KIF3A mRNA and protein expression levels were decreased in NSCLC. Furthermore, KIF3A knockdown promoted the proliferative, invasive and metastatic abilities, and suppressed the apoptosis of NSCLC cells. KIF3A was demonstrated to inhibit the occurrence and development of NSCLC by interacting with IFT57. In addition, low mRNA and protein expression levels of both KIF3A and IFT57 were associated with adverse survival times of patients with NSCLC. Collectively, these results suggested that KIF3A may function as a tumor suppressor in NSCLC and could be developed as a therapeutic target for the treatment of NSCLC.

Acknowledgements

Not applicable.

Funding

The present study was supported by grants from the Major Scientific and Technological Innovation Project of Shandong Province (grant no. 2018CXGC1212), the Science and Technology Foundation of Shandong Province (grant no. 2014GSF118084), the CSCO-QiLu Oncology Research Fund (grant no. Y-Q201802-014), the Medical and Health Technology Innovation Plan of Jinan City (grant no. 201805002) and the National Natural Science Foundation of China (grant no. 81372333).

Availability of data and materials

The datasets used and/or analyzed during the present study are available from the corresponding author upon reasonable request.

Authors' contributions

YQ and YY conceived and designed the present study. XL and RL performed the experiments. MZ and HW collected the clinical samples and analyzed the clinical data. YY and XL analyzed the data, performed the bioinformatic analysis and drafted the initial manuscript. All authors read and approved the final manuscript and agreed to be accountable for all aspects of the research.

Ethics approval and consent to participate

The present study was approved by the Ethics Committee of Qilu Hospital of Shandong University (Jinan, China; approval no. KYLL-2018-048). Patients or their families agreed and provided written informed consent.

Patient consent for publication

Not applicable.

Competing interests

The authors declare that they have no competing interests.

References

1. Bray F, Ferlay J, Soerjomataram I, Siegel RL, Torre LA and Jemal A: Global cancer statistics 2018: GLOBOCAN estimates of incidence and mortality worldwide for 36 cancers in 185 countries. *CA Cancer J Clin* 68: 394-424, 2018.
2. Gridelli C, Rossi A, Carbone DP, Guarize J, Karachaliou N, Mok T, Petrella F, Spaggiari L and Rosell R: Non-small-cell lung cancer. *Nat Rev Dis Primer* 1: 15009, 2015.
3. Boloker G, Wang C and Zhang J: Updated statistics of lung and bronchus cancer in United States (2018). *J Thorac Dis* 10: 1158-1161, 2018.
4. Kolpakova-Hart E, Jinnin M, Hou B, Fukai N and Olsen BR: Kinesin-2 controls development and patterning of the vertebrate skeleton by Hedgehog- and Gli3-dependent mechanisms. *Dev Biol* 309: 273-284, 2007.
5. Rosenbaum JL and Witman GB: Intraflagellar transport. *Nat Rev Mol Cell Biol* 3: 813-825, 2002.
6. Hirokawa N: Kinesin and dynein superfamily proteins and the mechanism of organelle transport. *Science* 279: 519-526, 1998.
7. Barakat MT, Humke EW and Scott MP: Kif3a is necessary for initiation and maintenance of medulloblastoma. *Carcinogenesis* 34: 1382-1392, 2013.
8. Liu Z, Rebowe RE, Wang Z, Li Y, Wang Z, DePaolo JS, Guo J, Qian C and Liu W: KIF3a promotes proliferation and invasion via Wnt signaling in advanced prostate cancer. *Mol Cancer Res* 12: 491-503, 2014.
9. Kim M, Suh YA, Oh JH, Lee BR, Kim J and Jang SJ: KIF3A binds to β -arrestin for suppressing Wnt/ β -catenin signalling independently of primary cilia in lung cancer. *Sci Rep* 6: 32770, 2016.
10. Travis WD, Brambilla E, Burke AP, Marx A and Nicholson AG (eds): WHO Classification of Tumours of the Lung, Pleura, Thymus and Heart. 4th edition. International Agency for Research on Cancer, Lyon, 2015.
11. Amin MB, Edge S, Greene F, Byrd DR, Brookland RK, Washington MK, Gershenwald JE, Compton CC, Hess KR, Sullivan DC, *et al* (eds): AJCC Cancer Staging Manual. 8th edition. Springer International Publishing, New York, NY, 2017.
12. Liu X, Li C, Yang Y, Liu X, Li R, Zhang M, Yin Y and Qu Y: Synaptotagmin 7 in twist-related protein 1-mediated epithelial-mesenchymal transition of non-small cell lung cancer. *EBioMedicine* 46: 42-53, 2019.
13. Livak KJ and Schmittgen TD: Analysis of relative gene expression data using real-time quantitative PCR and the 2(-Delta Delta C(T)) method. *Methods* 25: 402-408, 2001.
14. Gyorffy B, Surowiak P, Budczys J and Lanczky A: Online survival analysis software to assess the prognostic value of biomarkers using transcriptomic data in non-small-cell lung cancer. *PLoS One* 8: e82241, 2013.
15. Broglio KR and Berry DA: Detecting an overall survival benefit that is derived from progression-free survival. *J Natl Cancer Inst* 101: 1642-1649, 2009.
16. Mizuno H, Kitada K, Nakai K and Sarai A: PrognoScan: A new database for meta-analysis of the prognostic value of genes. *BMC Med Genomics* 2: 18, 2009.
17. Jensen LJ, Kuhn M, Stark M, Chaffron S, Creevey C, Muller J, Doerks T, Julien P, Roth A, Simonovic M, *et al*: STRING 8-a global view on proteins and their functional interactions in 630 organisms. *Nucleic Acids Res* 37: D412-D416, 2009.
18. Tang Z, Li C, Kang B, Gao G, Li C and Zhang Z: GEPIA: A web server for cancer and normal gene expression profiling and interactive analyses. *Nucleic Acids Res* 45: W98-W102, 2017.
19. Ghandi M, Huang FW, Jane-Valbuena J, Kryukov GV, Lo CC, McDonald ER III, Barretina J, Gelfand ET, Bielski CM, Li H, *et al*: Next-generation characterization of the cancer cell line encyclopedia. *Nature* 569: 503-508, 2019.
20. Irizarry RA, Bolstad BM, Collin F, Cope LM, Hobbs B and Speed TP: Summaries of affymetrix GeneChip probe level data. *Nucleic Acids Res* 31: e15, 2003.

21. Okayama H, Kohno T, Ishii Y, Shimada Y, Shiraishi K, Iwakawa R, Furuta K, Tsuta K, Shibata T, Yamamoto S, *et al*: Identification of genes upregulated in ALK-positive and EGFR/KRAS/ALK-negative lung adenocarcinomas. *Cancer Res* 72: 100-111, 2012.
22. Raponi M, Zhang Y, Yu J, Chen G, Lee G, Taylor JM, Macdonald J, Thomas D, Moskaluk C, Wang Y and Beer DG: Gene expression signatures for predicting prognosis of squamous cell and adenocarcinomas of the lung. *Cancer Res* 66: 7466-7472, 2006.
23. Wilkerson MD, Yin X, Hoadley KA, Liu Y, Hayward MC, Cabanski CR, Muldrew K, Miller CR, Randell SH, Socinski MA, *et al*: Lung squamous cell carcinoma mRNA expression subtypes are reproducible, clinically important, and correspond to normal cell types. *Clin Cancer Res* 16: 4864-4875, 2010.
24. Molina JR, Yang P, Cassivi SD, Schild SE and Adjei AA: Non-small cell lung cancer: Epidemiology, risk factors, treatment, and survivorship. *Mayo Clin Proc* 83: 584-594, 2008.
25. Wouters MW, Siesling S, Jansen-Landheer ML, Elferink MA, Belderbos J, Coebergh JW and Schramel FM: Variation in treatment and outcome in patients with non-small cell lung cancer by region, hospital type and volume in the Netherlands. *Eur J Surg Oncol* 36 (Suppl 1): S83-S92, 2010.
26. Barua S, Fang P, Sharma A, Fujimoto J, Wistuba I, Rao AUK and Lin SH: Spatial interaction of tumor cells and regulatory T cells correlates with survival in non-small cell lung cancer. *Lung Cancer* 117: 73-79, 2018.
27. Li Y, Deng L, Zhao X, Li B, Ren D, Yu L, Pan H, Gong Q, Song L, Zhou X and Dai T: Tripartite motif-containing 37 (TRIM37) promotes the aggressiveness of non-small-cell lung cancer cells by activating the NF-KB pathway. *J Pathol* 246: 366-378, 2018.
28. Guo X, Macleod GT, Wellington A, Hu F, Panchumarthi S, Schoenfield M, Marin L, Charlton MP, Atwood HL and Zinsmaier KE: The GTPase dMiro is required for axonal transport of mitochondria to *Drosophila* synapses. *Neuron* 47: 379-393, 2005.
29. Geng G, Du Y, Dai J, Tian D, Xia Y and Fu Z: KIF3A knockdown sensitizes bronchial epithelia to apoptosis and aggravates airway inflammation in asthma. *Biomed Pharmacother* 97: 1349-1355, 2018.
30. Lee J, Oh DH, Park KC, Choi JE, Kwon JB, Lee J, Park K and Sul HJ: Increased primary cilia in idiopathic pulmonary fibrosis. *Mol Cells* 41: 224-233, 2018.
31. Taschner M and Lorentzen E: The intraflagellar transport machinery. *Cold Spring Harb Perspect Biol* 8: a028092, 2016.
32. Prevo B, Scholey JM and Peterman EJG: Intraflagellar transport: Mechanisms of motor action, cooperation, and cargo delivery. *FEBS J* 284: 2905-2931, 2017.
33. Nakayama K and Katoh Y: Ciliary protein trafficking mediated by IFT and BBSome complexes with the aid of kinesin-2 and dynein-2 motors. *J Biochem* 163: 155-164, 2018.
34. Funabashi T, Katoh Y, Okazaki M, Sugawa M and Nakayama K: Interaction of heterotrimeric kinesin-II with IFT-B-connecting tetramer is crucial for ciliogenesis. *J Cell Biol* 217: 2867-2876, 2018.



This work is licensed under a Creative Commons Attribution-NonCommercial-NoDerivatives 4.0 International (CC BY-NC-ND 4.0) License.